Applied Catalysis B: Environmental 115–116 (2012) 63–73

Contents lists available at SciVerse ScienceDirect

Applied Catalysis B: Environmental

journal homepage: www.elsevier.com/locate/apcatb

Gas-phase hydrodeoxygenation of guaiacol over Fe/SiO_2 catalyst

R.N. Olcese[a], M. Bettahar[b], D. Petitjean[a], B. Malaman[c], F. Giovanella[a], A. Dufour[a,*]

[a] LRGP, UPR CNRS, ENSIC, 1 rue Grandville, BP20451, 54001 Nancy Cedex, France
[b] SRSMC, UMR CNRS – Nancy Université, Bd. des Aiguillettes 54506 Vandœuvre-lès-Nancy, France
[c] IJL, UMR CNRS-Nancy Université-UPMV, Faculté des Sciences, Bd. des Aiguillettes 54506 Vandœuvre-lès-Nancy, France

ARTICLE INFO

Article history:
Received 19 October 2011
Received in revised form
29 November 2011
Accepted 3 December 2011
Available online 9 December 2011

Keywords:
Green chemicals
Aromatic
Lignin
Bio-oils
Hydrotreatment
Catalyst
Iron

ABSTRACT

Lignin could be an important green source for aromatic hydrocarbon production (benzene, toluene and xylenes, BTX). Catalytic hydrodeoxygenation (HDO) of guaiacol was studied over Fe/SiO_2 as a model reaction of lignin pyrolysis vapours hydrotreatment. The catalytic conditions were chosen to match with the temperature of never-condensed lignin pyrolysis vapours. The catalyst was characterised by XRD, Mössbauer spectroscopy, N_2 sorption and temperature programmed oxidation. A comparison is made with a commercial cobalt-based catalyst. Cobalt-based catalyst shows a too high production of methane. Fe/SiO_2 exhibits a good selectivity for BT production. It does not catalyse the aromatic ring hydrogenation. Temperature (623–723 K) and space time (0.1–1.5 g_{cat} h/g_{GUA}) influence the aromatic carbon–oxygen bond hydrogenolysis reaction whereas H_2 partial pressure (0.2–0.9 bar) has a minor influence. 38% of BT yield was achieved under the best investigated conditions. Reaction mechanisms for guaiacol conversion over Fe/SiO_2 are discussed.

1. Introduction

Lignin is a natural polymer of methoxylated phenylpropane units and it is the second most important compound in lignocellulosic biomass (about 25 wt.%) [1]. It is industrially available at low prices from cellulose pulping processes (fuel value of about $0.04 per pound on a dry basis depending on the technical–economical scenario) [2]. Lignin is today mainly converted to heat and/or power by combustion. Lignin valorisation into aromatic hydrocarbons (benzene, toluene and xylene, BTX) represents a key route for lignocellulosic biorefinery (see Fig. 1) [1–4].

BTX are widely used as fuel additives and solvents and are starting blocks for several molecules [1,2,5]. Conventional technologies for BTX production are: naphtha reforming (C_6–C_{12}; over Pt/Al_2O_3), C_2–C_6 paraffins conversion on Gallium promoted ZSM-5, coal pyrolysis and methanol-to-gasoline Mobil process on ZSM-5.

Catalytic pyrolysis was proposed as a single-step lignin conversion process [6–11]. The catalyst is mixed with lignin before pyrolysis. Different lignins were mixed and pyrolysed with NH_3-treated H-ZMS-5 or $CoO\text{-}MoO_3/Al_2O_3$ in a pyroprobe [8]. With the zeolite catalyst lignin is first cracked and deoxygenated to C_2–C_6 olefins which then are converted into BTX. With $CoO\text{-}MoO_3/Al_2O_3$ catalyst, lignin is thought to depolymerise to phenols, and then phenols are deoxygenated on $CoO\text{-}MoO_3$ sites to aromatic hydrocarbons [8].

One of the main drawbacks of the direct catalytic pyrolysis is the difficulty to recover and regenerate the catalyst (mixed with the char) [12]. Moreover, catalytic pyrolysis involves many physical–chemical phenomena that are difficult to be monitored in the same reactor.

Lignin can also be valorised in two-step processes consisting in a depolymerisation of lignin and a treatment of depolymerised lignin (lignin bio-oil). Several techniques were proposed for lignin depolymerisation: pyrolysis, liquefaction (with a huge variety of solvents and catalysts), oxidation, electrochemical treatments, etc. [1]. Pyrolysis and liquid phase hydrogenation were the most studied [1]. Liquid phase hydrogenation consists on the high pressure (50–100 bar, 523–723 K) treatment of lignin in a solvent like an aliphatic alcohol, water [13,14] or phenol [15,16] under H_2 and/or a hydrogen donor (like tetralin). The main disadvantages of liquid treatments are: the consumption of solvent, the cost of high pressure equipment and the difficulties to separate catalyst, char, products, solvent and non-reacted lignin from the reaction media. Lignin pyrolysis produces permanent gases (H_2, CO, CO_2, CH_4), a fluffy char and a complex mixture of condensable compounds rich in OMACs (oxygenated monoaromatic compounds) [12,17–19]. Faix et al. [20] studied the products of the non-catalytic pyrolysis of lignin at 600 °C in a fixed bed reactor. 15–30 wt.% of OMACs was obtained using different lignins.

* Corresponding author.
E-mail address: anthony.dufour@ensic.inpl-nancy.fr (A. Dufour).

0926-3373/$ – see front matter © 2011 Elsevier B.V. All rights reserved.
doi:10.1016/j.apcatb.2011.12.005

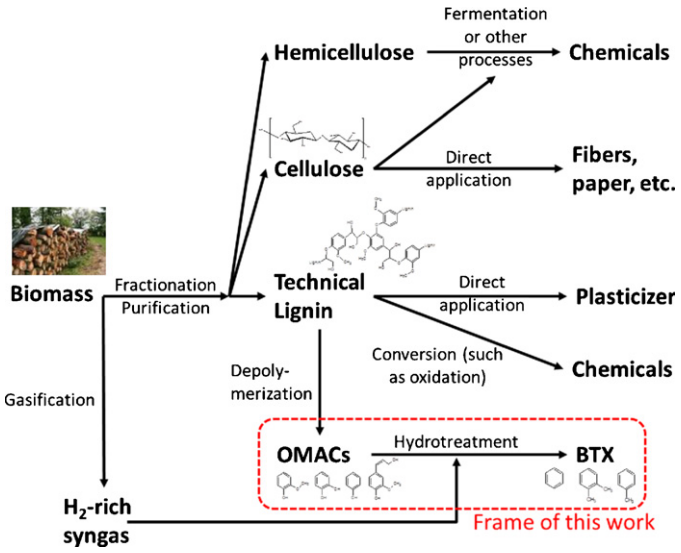

Fig. 1. A possible ligno-cellulosic biorefinery (adapted from [4]). OMACs: oxygenated mono-aromatic compounds.

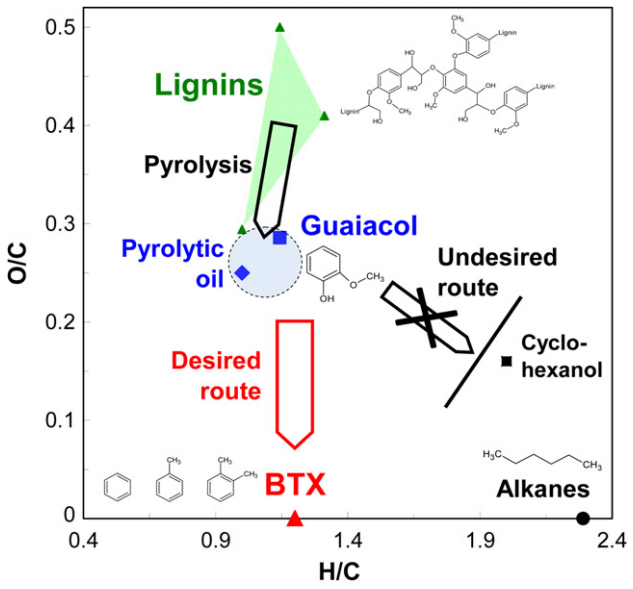

Fig. 2. Van Krevelen diagram of lignin hydrotreatment (based on [12]). Pyrolytic oil was obtained by de Wild et al. on a fluidised bed [12]. The green triangle involves roughly all kinds of lignin [33]. (For interpretation of the references to colour in this figure legend, the reader is referred to the web version of the article.)

The catalytic conversion of lignin pyrolysis oils (or model compounds like guaiacol) was extensively investigated in the liquid phase under H_2 high pressure [12,13,21–23]; and in the gas phase with H_2 [24–30] or without H_2 [31].

OMACs are generated in the gas phase during lignin pyrolysis in a reactor set at a temperature of about 773 K [17–19,32]. Once condensed, the re-evaporation of bio-oils is difficult since bio-oils are very reactive and cause fouling of pipes. In addition, working on the liquid phase requires high pressures (that means costly equipment) and the condensation step after pyrolysis is detrimental for the heat recovery of the entire process [17]. For these reasons, the vapour phase hydrotreatment of OMACs before condensation seems a better route.

This paper is a contribution on the hydrodeoxygenation (HDO) of OMACs, using guaiacol as a model compound. Guaiacol is a minor but significant component in a very complex mixture in lignin bio-oils [32]. It has been chosen as a model compound because its elemental composition is close to the overall elemental composition of lignin bio-oils (see H/O/C ratios in Fig. 2) and its hydroxyl and methoxyl functions on the aromatic ring are significant and key functions for aromatics species in lignin bio-oil.

The hydrogenation should be soft in order to favour BTX production at the expense of the ring hydrogenation (Fig. 2). The catalyst should act selectively towards the hydrogenolysis of the oxygen–aromatic bonds of hydroxyl or methoxyl functions, i.e. it should be able to activate molecular hydrogen and the C(aromatic)—O bond. Moreover, it should be resistant to lignin pyrolysis products and have the desired aspects of any catalyst: low price, low deactivation, easy regeneration and environmentally friendly disposal.

Phenol could also be an interesting product, but allowing some oxygen atoms linked to aromatic ring could produce an endless list of isomers difficult to be separated from the different compounds in bio-oils. Consequently, in our opinion, a complete hydrodeoxygenation to BTX seems a better route instead of a partial HDO to phenols.

Whilst undertaking our work, few papers appeared on the subject using similar reaction conditions but different catalysts (Ni_2P/SiO_2, Fe_2P/SiO_2, MoP/SiO_2, Co_2P/SiO_2 and WP/SiO_2 [24]; CoMoS over alumina, zirconia or titania [25,26]; Pt-Sn/CNF [29]). Aims and practical results of these papers are discussed in this manuscript. From the academic point of view, they indicated that the catalysts activity and selectivity strongly depend on the nature of the active phase and that of the support. These factors particularly influence the two main competitive reactions, namely the HDO and the aromatic ring hydrogenation.

Transition (Fe, Co, Ni) and precious metals (Pt, Pd, Ru, Rh, Ir, etc.) are known to catalyse hydrogenation [34], but unfortunately most of them also catalyse benzene hydrogenation in the temperature range 473–673 K [35]. Emmett and Skau [34] detected no activity for benzene hydrogenation at 673 K working with Fe. Lately, Yoon and Vannice [35] measured a relatively low activity of Fe for benzene hydrogenation compared to other transition or precious metals (Ni, Co). Fe is a trade-off between activity and selectivity. This is the reason why we chose iron as the active phase in the guaiacol HDO, expecting minimum aromatic ring hydrogenation.

Metal–support interactions and support acidity play a crucial role in complex chemistry of transition metal supported catalysts. It was studied for hydrogenation of aromatics hydrocarbons [36–40] as well as for aromatic alcohols [25,26,41–45]. Benzene is hydrogenated with higher rates on Ni catalysts when silica was used as a support instead of alumina [45]. For HDO reaction on supported Mo catalysts, alumina gave higher activity but rapid deactivation due to coke deposit [41,42,45]. In contrast, the use of the less acidic active carbon led to lower activity but a better selectivity in HDO products [41,43–45]. We concluded that silica would be a good iron carrier due to its low acidity.

Cobalt was chosen for comparison. Cobalt is an inexpensive active phase compared to precious metals. It is a component of typical $CoMoS/Al_2O_3$ hydrotreating catalyst and it is active for HDO [46]. Our group performed a screening of catalyst at 623 K [47]. It was shown that cobalt is able to catalyse the production of BT from guaiacol.

For those reasons, our work focuses on the gas phase HDO of guaiacol to BTX as a model compound of lignin pyrolysis vapours using Fe/SiO_2 and Co/Kieselguhr catalysts, at the temperature of interest (623–723 K) for coupling the HDO catalytic reactor to the pyrolysis reactor. The catalysts were characterised by BET, XRD, Mössbauer spectroscopy and temperature programmed oxidation (TPO).

2. Material and method

2.1. Thermodynamic analysis

The chemical equilibrium was studied with GASEQ [48]. 31 compounds were defined: phenols (phenol, cresols, catechols, and guaiacol), ring hydrogenated (cyclohexane, cyclohexene, cyclohexanol, etc.), HDO products (BTX), PAHs, carbon, methanol, water, carbon dioxide and monoxide and alkanes (from methane to C_6). Many compounds were not pre-defined on GASEQ library. Their properties (ΔH_f°, ΔG_f° and $Cp_{(T)}$) were calculated using THERGAS [49] (based on tabulated data or Benson's method). Starting data were 1% guaiacol, 90% H_2, 9% Ar, 1 atm and 673 K.

2.2. Experimental

2.2.1. Preparation of catalyst

Iron over silica (Fe/SiO_2) catalyst was prepared by simple impregnation. 12 g of silica (Aerosil 130, Degussa) were contacted with 65 ml of an iron nitrate nonanhydrate (Sigma) solution in deionised water (0.2 g/ml). The mixture was exposed to vacuum at room temperature for 3 h, and then dried 24 h at 373 K. The resulting impregnated solid was grounded and sieved (100–160 μm), and then calcined at 773 K under Argon flow (50 Nml/min) for 1 h. A test iron-free silica sample was prepared repeating the same procedure but using deionised water instead of iron nitrate solution.

The calcinated catalyst was reduced in situ by pure H_2 (50 ml/min) before guaiacol HDO. Temperature was increased from 298 K to 773 K at a rate of 5 K/min, then hold 773 K during 60 min. The reactor feed was then changed to hydrogen–argon mix at desired flows and H_2 molar fraction and the temperature was set to the reaction temperature. After a stabilisation time (60 min), guaiacol syringe pump was turn on.

The Cobalt on Kieselguhr catalyst (Co/Kies) was supplied from Strem Chemicals. It was grounded, sieved and reduced under the same conditions as the iron-based catalyst.

2.2.2. Guaiacol catalytic HDO experiments

Catalytic tests were made in a continuous flow fixed-bed reactor (d = 4.1 mm) at atmospheric pressure (Fig. 3). A known mass of catalyst (30–200 mg) was placed into a quartz reactor. The reactor was heated with an electrical furnace. Reaction temperature

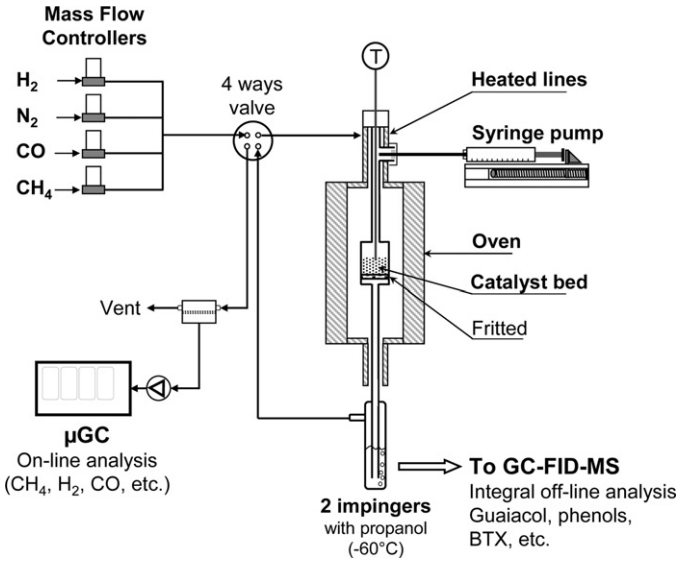

Fig. 3. Scheme of the experimental set-up for catalytic conversion of biomass pyrolysis tar model compounds.

Table 1
Experimental conditions investigated in this paper.

Catalyst type	Temperature (K)	H_2 partial pressure (bar)	1/WHSV (h) ($g_{catal}/(g_{guaiacol}/h)$)
Fe/SiO_2	623, 673[a], 723	0, 0.2, 0.5, 0.9[a]	0.11, 0.38[a], 0.79, 1.50
Co/Kieselguhr	673	0.9	0.49, 0.70, 0.81

[a] Nominal conditions.

was measured with a thermocouple placed inside the reactor and set at 623, 673 or 723 K. The gas flow rates (Ar, H_2) were controlled with mass flow controllers (MFC, Bronkhorst). Mass residence time ($1/WHSV = g_{catalyst}/(g_{GUAIACOL}/h)$) was changed by the variation of catalyst mass. The inlet line of the reactor was heated (473–523 K). At this stage guaiacol was injected and vaporised with a syringe pump (43–172 μl/h). All experiences were done at 1 vol.% of guaiacol. About 1000 μmol of guaiacol was injected on the catalyst bed for nominal conditions (Fe/SiO_2, 673 K, 1/WHSV = 0.38 h, 30 min time on stream). In a standard run, gas flow, liquid flow and catalyst mass were 73 Nml/min H_2, 7.5 Nml/min Ar, 239 μl/h Guaiacol and 100 mg, respectively.

Table 1 displays the operating conditions studied in this work. The screening of catalyst performances needs short times on stream due to the rapid deactivation by coking, inherent of this reaction (see for instance reference [30]).

The outlet of the reactor was also heated (473 K) to avoid any condensation of products and guaiacol. The heated exit pipe was connected to 2 impingers filled with about 15 ml of isopropanol (cooled at 213 K) where condensable products were collected. The authors are aware of the tar protocole [50,51]. The sampling efficiency of the 2 impingers was checked by analysing the 2nd impinger [51] and by the μ-GC analysis (see below).

50 μl of internal standard (1-undecene) was injected in the entire impingers solution volume at the end of the experiment. Condensable products were first identified off-line by GC–MS analysis and then quantified by GC–FID on a 1701 (60 m, ID 0.25 mm, 0.25 μm) column, with a split division ratio of 1/30. The GC heated program was as follow: 313 K for 5 min, 5 K/min to 423 K, 10 K/min to 543 K then hold 5 min. Relative response factors were calculated from pure compounds, with very good reproducibility (relative standard deviation of 3 injections lower than 5% for each products). Reactant and product concentrations at the exit were calculated dividing GC data on the time on stream.

Incondensable products (methane, ethane, CO, CO_2, etc.) were analysed on-line with a μGC-Varian 490 equipped with four modules connected to the exit of the impingers. The four modules were composed of two molecular sieves 5A, a PoraPlot U and a CP–Wax 52CB columns. μGC-490 signal was calibrated using four standard bottles (Air Liquide, France). It allows quantifying BTX on-line at concentration lower than 10 ppm every 3 min. No BTX signal was detected at the outlet of the impingers thus confirming the good condensation of BTX and phenolic products in the impingers. μ-GC on-line data was first integrated and then divided on the time on stream to calculate the average flow rate of permanent gases.

2.2.3. Characterisations of the catalyst

The load in iron of the Fe/SiO_2 catalyst was checked by ICP-MS analysis (CNRS-SARM procedure [52]) and was 17% (w/w). Co/Kieselguhr cobalt load was 25% (w/w).

Specific surface areas of catalysts were calculated from sorption isotherms of nitrogen at 77 K, using BET method. Isotherms were obtained with a Sorptomatic 1990 (Thermo Finnigan, Waltham, MA, USA). All the samples were previously outgassed at 523 K for several hours.

The samples have been analysed by conventional X-ray powder analysis (XPERT Pro Cu Kα) and the crystal structures have been refined using the Fullprof software [53].

The ^{57}Fe Mössbauer measurements were carried out using a constant-acceleration spectrometer in standard transmission geometry with a ^{57}CoRh source (25 mCi). Spectra were recorded at 300 K. A polycrystalline absorber with natural abundance of ^{57}Fe isotope and thickness of about 15 mg cm^{-2} was used. The Mössbauer spectra were fitted with a least-squares method program assuming Lorentzian peaks [54].

TPO was performed on the used catalyst using the same reactor as for guaiacol catalytic conversion. 60 mg of sample were flowed by air (50 Nml/min) and temperature was increased from 293 to 1073 K at 3 K min^{-1}. Produced carbon dioxide was measured online by the μGC. Carbon monoxide was not detected.

2.3. Definitions

Carbon yields (Y_C%) were calculated using Eq. (1) where N_j^i is the number of j (C, O, H) atoms per *molecule*, i (guaiacol, anisole, etc.). n_i (mole) is the amount of i product at the exit of the reactor and $n_{GUA}{}^{\circ}$ (mole) is the amount of guaiacol moles introduced in the reactor. HDO conversion (X_{HDO}%) was calculated using Eq. (2) (PhOH: phenol; ANI: anisole; MePhOH: cresols; GUA: guaiacol; Cat: catechol; MeCat: methyl catechol).

H/C* and O/C* of products were calculated by Eqs. (3) and (4), respectively. O/C* was defined to be equal to zero if a complete HDO is achieved to produce H_2O. H/C* is equal to 1.14 if guaiacol is completely converted into toluene. Under this condition, guaiacol HDO is optimal. If the carbon atom of guaiacol are completely hydrogenated into CH_4, H/C* is equal to 4.

$$Y_C^i\% = 100 \cdot \frac{(N_C^i)\cdot(n_i)}{(N_C^{GUA})\cdot(n_{GUA}{}^{\circ})} \quad (1)$$

$$X_{HDO}\% = 100 \cdot \left(1 - \frac{(n_{PhOH} + n_{ANI} + n_{MePhOH} + 2\cdot(n_{GUA} + n_{Cat} + n_{MeCat}))}{2\cdot(n_{GUA}{}^{\circ})}\right) \quad (2)$$

$$H/C^* = \sum_i \left(\frac{N_H^i}{N_C^i}\right)\cdot\frac{Y_C^i\%}{100} \quad (3)$$

$$O/C^* = \sum_i \left(\frac{N_O^i}{N_C^i}\right)\cdot\frac{Y_C^i\%}{100} \quad (4)$$

3. Results

3.1. Thermodynamic analysis of the reactive system

Some key reactions were analysed in THERGAS [49] to determine the variation of the free Gibbs energy as a function of the temperature. The key reactions (R1–R6) are given in Table 2 and their free Gibbs energy in Table 3.

Table 3 shows that the goal reactions (R1 and especially R2) are possible on the entire range of temperature. The selectivity of BTX formation from phenols HDO should be consequently optimised by a suitable kinetic approach. The formation of saturated rings (R3 or R5) is not favoured from 700 K. Reactions R4 and R6 are favoured at higher temperatures. CH_4 would be the final product if the thermodynamic equilibrium is achieved considering the 31 possible compounds. This result is trivial since methane is the most stable molecule at this temperature.

Table 2
Key reactions selected to assess the thermodynamic of guaiacol HDO.

Guaiacol + $2H_2$ = benzene + H_2O + methanol	R1, HDO conversion of guaiacol to benzene
Guaiacol + $2H_2$ = toluene + $2H_2O$	R2, HDO conversion of guaiacol to toluene
Guaiacol + $4H_2$ = cyclohexanol + methanol	R3, hydrogenation of the guaiacol aromatic ring
2Guaiacol + $3H_2$ = diphenyl + 2 methanol + $2H_2O$	R4, polymerisation reaction
Benzene + $3H_2$ = cyclohexane	R5, hydrogenation of benzene
Benzene = $3H_2$ + 6C	R6, pyrolysis of benzene with coke production

3.2. Blank tests, reproducibility and mass transfer limitations

Homogeneous conversion of guaiacol was checked to be negligible below 723 K for our empty reactor. An experience with the non-impregnated iron-free silica also showed no conversion. The nominal experiment (90% H_2, 673 K, 0.38 g_{cat} h/g_{GUA}, Fe/SiO_2) was repeated five times. A good reproducibility was achieved. Relative standard deviation of guaiacol conversion was 4% and 5.5% for product distribution. Guaiacol conversion was 70%.

Carbon balances were between 84% and 92% without the carbonaceous deposit on the catalyst. The carbonaceous deposit quantified by TPO was 7% for nominal conditions (see below). Total carbon balance (GC analysed species + coke deposit) was 94% (for nominal conditions).

Major products detected by GC/MS in the impingers' solution were: phenol, cresols, anisole, benzene, toluene, and methanol. Methylcatechol was also detected. Our GC method allows to measure methanol only roughly. Methanol concentration on exit gas was about 0.04 vol.% for nominal conditions.

In order to rule out the external mass transfer limitations, experiences were done by varying the mass of catalyst in the range 30–210 mg, but tailoring reactant flow to maintain a stable 1/WHSV of 0.38 h. No variation of guaiacol conversion or products yields was found.

We did not succeed to investigate experimentally the internal mass transfer because of a too high pressure drop inside the bed for smaller particles. The internal mass transfer limitation was ruled out using the modified Thiele or Weisz modulus (as in [55]). The modified Thiele modulus allows comparing a reaction-induced flow rate to a diffusion flow rate when the true intrinsic reaction kinetics (order and kinetic constant) are unknown and when only the flow of consumed reagent is available. The details of calculation are given in the supplementary material. The modified

Table 3
Variation of free Gibbs energy of some key reactions (defined in Table 2) involved during guaiacol HDO.

Temperature (K)	ΔG (kcal mol^{-1})					
	R1	R2	R3	R4	R5	R6
400	−32.72	−50.4	−27.57	−60.22	−14.3	−34.99
500	−33.39	−51.18	−18.54	−61.45	−5.18	−39.22
600	−33.89	−51.85	−9.25	−62.47	4.17	−43.63
700	−34.26	−52.43	−0.18	−63.31	13.6	−48.17
800	−34.53	−52.93	9.71	−64.01	23.07	−52.79
900	−34.71	−53.36	19.27	−64.6	32.53	−57.47
1000	−34.83	−53.75	28.85	−65.08	41.97	−62.19

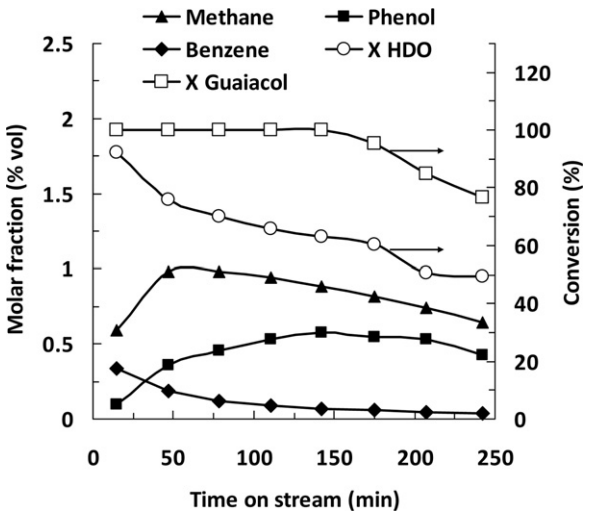

Fig. 4. Evolution of the gases molar fraction and of guaiacol and HDO conversions as a function of time on stream (Fe/SiO_2, $T = 673$ K, $P = 1$ atm, 90% H_2, 1 vol.% guaiacol, 9% Ar, 1/WHSV = 1.50 g_{cat} h/g_{GUA}).

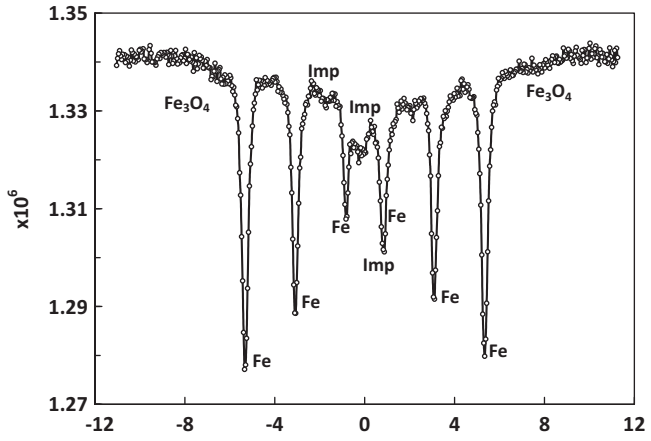

Fig. 5. Mössbauer spectrum of the used catalyst (after 4 h time on stream, Fig. 4). Imp: impurities (see text).

Thiele modulus was below 0.4 for all the investigated conditions. The experiments were thus conducted under the chemical regime.

3.3. Evolution of the reaction as a function of time on stream

Fig. 4 shows the evolution of guaiacol conversion, HDO conversion and main products with time on stream. Conditions for a high conversion of guaiacol but with a HDO conversion of about 60% was chosen to compare our results with published data [24,27,29,30]. The aim of this paper is not to investigate the kinetic of primary guaiacol conversion (that needs low guaiacol conversion) but rather the evolution of benzene selectivity as a function of time on stream. Since the desired BTX products come from secondary reactions, their productions in appreciable yields need a high guaiacol conversion in primary products (phenols, etc.) and secondary conversion of these primary products. It is indeed of great interest to investigate the stability of the catalyst on BT selectivity and not only on guaiacol conversion.

The main product gases were methane and carbon monoxide. Ethylene, ethane and carbon dioxide were also detected by the μGC but at molar fractions lower than 0.015 mol%.

CH_4 can be formed from methoxyl function decomposition and ring hydrogenation. CH_4 mole fraction stays below 1 mol% (1 mol of CH_4 formed for 1 mol of guaiacol at 1 vol.%). This finding suggests that there is very little ring hydrogenation. CO could be formed from phenol dehydroxylation. Aromatic ring dehydroxylation could form coke precursors (PAH through cyclopentadienyl radical) [56,57].

A decrease in guaiacol and HDO conversion is observed due to the catalyst deactivation that will be explained by the characterisation of the catalyst.

3.4. Catalyst characterisation

Specific surface area of fresh calcinated catalyst was 116 m^2/g close to 130 m^2/g of the original silica. This result shows that our impregnation method does not reduce significantly the porous structure of silica. Used catalyst (under nominal conditions) showed almost the same specific surface (118 m^2/g). This finding is consistent with very few diffusion limitations in the pores [55]. Co/Kieselguhr specific surface was 38 m^2/g.

XRD patterns (see Fig. S.1. in supplementary material) confirmed the presence of α-Fe as major phase before and after reaction as showed by the signals $2\theta = 44.6°$, 64.9° and 83.4° [58,59]. The crystallite size evaluated for 110 lines (2θ of 45°) of iron (Fullprof software procedure [53]) indicated that the average size of crystallites was about 10 nm. Other minor peaks on XRD patterns of spent catalyst could be explained by the presence of magnetite (Fe_3O_4, $2\theta = 35.5°$ and 62.9°) and/or maghemite (Fe_2O_3, $2\theta = 35.75°$ and 63.14°). Iron oxides are a minor phase after reduction and after guaiacol conversion. The reduced catalyst (before guaiacol conversion) was shown to be pyrophoric and thus difficult to be analysed. The silica gives a diffusion signal at small angles. Co/Kieselguhr commercial catalyst was found to be amorphous.

The Mössbauer spectrum of the spent catalyst (Fig. 5, after 4 h of guaiacol conversion, after Fig. 4) clearly shows a sextet characteristic of α iron (H = 331(1) kOe, IS = 0.00(1) mm/s, EQ = 0.00(1) mm/s, gamma = 0.31(1) mm/s). Several small contributions that could be addressed to cementite (Fe_3C, formed by Fe carburisation) and magnetite are also observed. The respective area of the sextet and the peaks of impurities are estimated to about 85, 3 and 12% for αFe, Fe_3O_4 and the carbide phase, respectively. These results are in fair agreement with the XRD pattern where metallic iron as a major phase and magnetite Fe_3O_4 as a very minor phase are observed yielding the carbide compound to be probably amorphous. Moreover, the magnetically ordered state observed for these three compounds in the Mössbauer spectrum implies that the particles was not in superparamagnetic domain. Therefore, their sizes of particles are in fair agreement with those deduced from the X-ray pattern since a superparamagnetic behaviour for αFe, Fe_3O_4 and (Fe,C) compounds occur for sizes below around 2 and 10 nm for Fe and the two others phases, respectively [54].

The active phase (α-Fe) stays the major phase even after 4 h of guaiacol HDO with no dramatic change in size and magnetite or carbide species formed in negligible amounts. This finding strongly suggests that the deactivation mechanism would mainly take place through coke deposition instead of iron carbide or oxide formation. Further work will deal with the effect of steam (and other pyrolysis gas) on the surface cleaning.

Analysis (by XRD and Mössbauer) of spent catalysts after 3 months of storage also shows a slow oxidation of the catalyst if stored at room conditions but reduced iron remains the major phase.

BET measurements showed that specific surface area of the used catalyst was almost the same as that of the fresh catalyst. Consequently, coke deposition does not plug significantly the pore mouths.

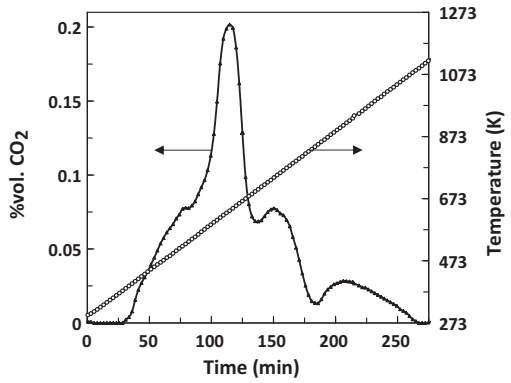

Fig. 6. Evolution of CO_2 formation during temperature programmed oxidation of used Fe/SiO_2 (after nominal conditions).

Coke deposit was investigated by means of TPO. TPO profile of the carbonaceous compounds is shown on Fig. 6. It exhibits three peaks at 634 (major peak), 741 and 924 K and a shoulder at 527 K corresponding to different coke species, most probably including coke precursors (PAH), solid amorphous (not seen by XRD) carbon formed from the PAH and iron carbide (analysed by Mössbauer). The nature and number of coke species depend on the nature of the catalyst. Zhu et al. [30] performed a similar study on Pt/SiO_2 and Pt/HBeta zeolite catalyst after anisole hydrotreatment. They found two peaks on silica supported catalyst and three peaks on zeolite supported catalyst. They explained that coke oxidation could be catalysed by platinum.

Valle et al. [60] studied coke formed during gas-phase upgrading of wood bio-oils on HZMS-5. Two peaks were obtained on the TPO curves. They explained that the first peak came from thermal decomposition of bio-oils, and the second peak came from catalytic reaction.

The integral of CO_2 production during TPO represented 7% of the carbon balance, which is consistent with the fact that products measured by GC and μ-GC accounted of around 85% (see Fig. S.2. in supplementary material) of the carbon balance. The overall carbon balance is thus closed to about 94%. Coke production was 6.6% g of coke/g of converted guaiacol in nominal conditions. Coke deposit level depends on several factors, amongst them the nature of the metal catalyst and of the oxygenated reactant molecule. The amount of carbon deposit is thus lower for Pt/SiO_2 (3.0% g coke/g of converted anisole) [30] but anisole was the HDO model compound. Anisole is a less oxygenated compound easier to be hydro-deoxygenated than guaiacol.

TPO quantification of coke deposit upon time on stream was not investigated. However, the "GC carbon balance" (moles of carbon analysed by GC in aromatics and in permanent gases at the outlet/moles of carbon injected in guaiacol) was stable and close to 85% for the entire time-on-stream (4 h) (see Fig. S.2. in supplementary materials). This suggests that coke deposition does not increase with time on stream due to lower guaiacol and HDO conversions upon time on stream.

3.5. Catalytic activity

3.5.1. Effect of H_2 partial pressure

The effect of hydrogen partial pressure on conversion and yields was investigated at 673 K (Fig. 7).

The conversion of guaiacol on Fe/SiO_2 in the absence of hydrogen differed clearly from any hydrotreatment experiences evidencing the role of hydrogen in the reaction. Guaiacol conversion was 30% without H_2, compared with 70% for pH_2 of 0.2 bar. However, the effect of hydrogen became negligible for 0.2–0.9 bar of H_2.

In the absence of hydrogen almost no HDO product were trapped in the impringers (except about 10% of anisole + cresols). Non-condensable gases were also produced in very little amounts. Carbon balance (without coke) was 70% for the experience without hydrogen, whilst it was between 84% and 92% for all the other experiences. This indicates important carbon deposit in the former case. One important role of hydrogen is to reduce the formation of coke precursors (probably PAH from phenol conversion). H_2O could be a reaction product of HDO and is also present in the pyrolysis gas. H_2O could also prevent the accumulation of coke by steam gasification [30]. The effect of H_2O partial pressure on coke deposition will be presented in future papers.

X_{HDO}% remains almost unchanged in the range 0.2 bar < pH_2 < 0.9 bar. Benzene and toluene yields increase slightly with hydrogen partial pressure at the expense of phenol and cresols (Fig. 7). The conversion of guaiacol into BT is reduced in a very little extent with the decrease of H_2 partial pressure. Carbon balance (without coke) was stable (0.2 bar < pH_2 < 0.9 bar) indicating that coke deposit on catalyst was not formed in a higher yield if H_2 partial pressure decreased from 0.9 to 0.2 bar.

These findings are quite important and show that the conversion of lignin vapours into BTX would even be possible if the gas stream is relatively poor in hydrogen. Fe/SiO_2 is a versatile catalyst towards H_2 partial pressure.

Shin and Keane [61] studied the effect of the partial pressure of hydrogen on the formation of cyclohexanol from phenol conversion at 573 K on Ni/SiO_2. They found that the reaction rate increases with H_2 concentration but benzene selectivity was essentially independent of hydrogen concentration, which is roughly consistent with our results (Fig. 7). The effect of hydrogen pressure on guaiacol hydrogenation was also reported for Pt/Al_2O_3 catalyst or HY zeolite [62]. In the presence of hydrogen both isomerisation and

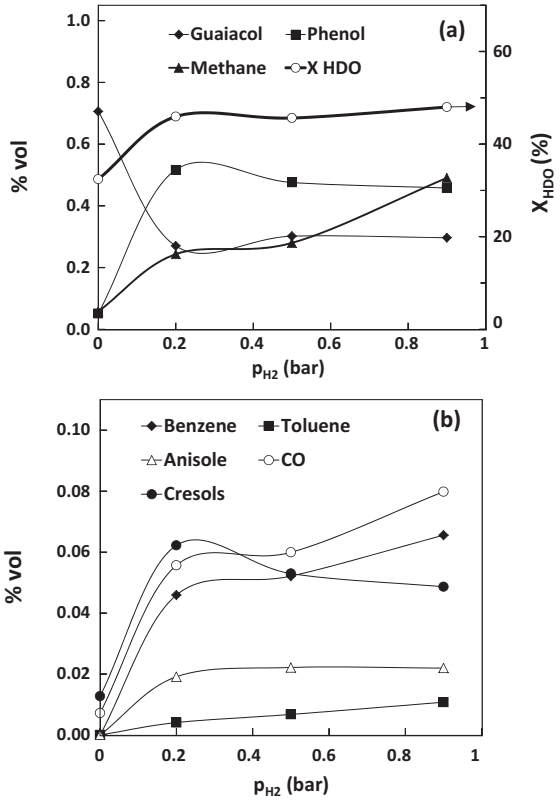

Fig. 7. Effect of H_2 partial pressure on (a) molar fraction of non-reacted guaiacol and major products and on HDO conversion (see Eq. (2)), (b) molar fraction of minor products (Fe/SiO_2; 673 K; 1 bar, 0.38 g_{cat} h/g_{GUA}).

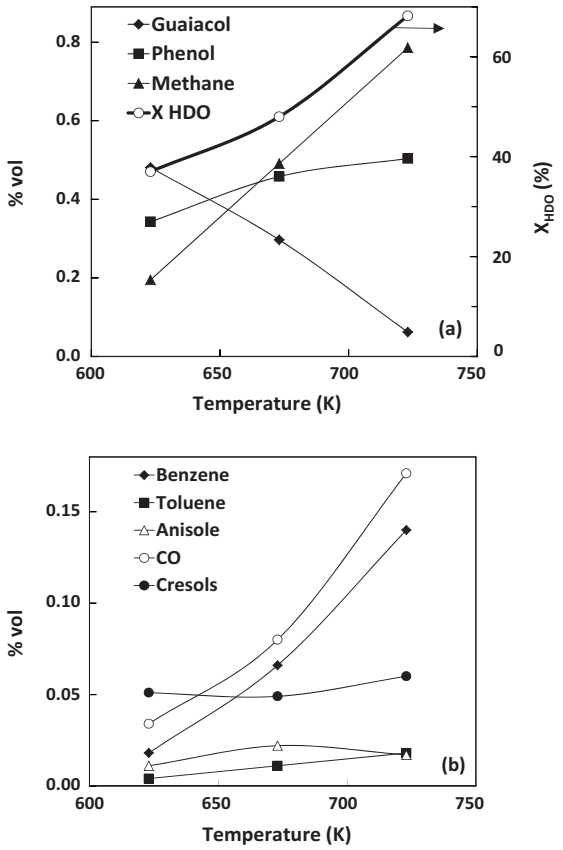

Fig. 8. Effect of temperature on (a) molar fraction of non-reacted guaiacol and major products and on HDO conversion (see Eq. (2)), (b) molar fraction of minor products (Fe/SiO_2; pH_2 = 0.9 bar; 0.38 g_{cat} h/g_{GUA}).

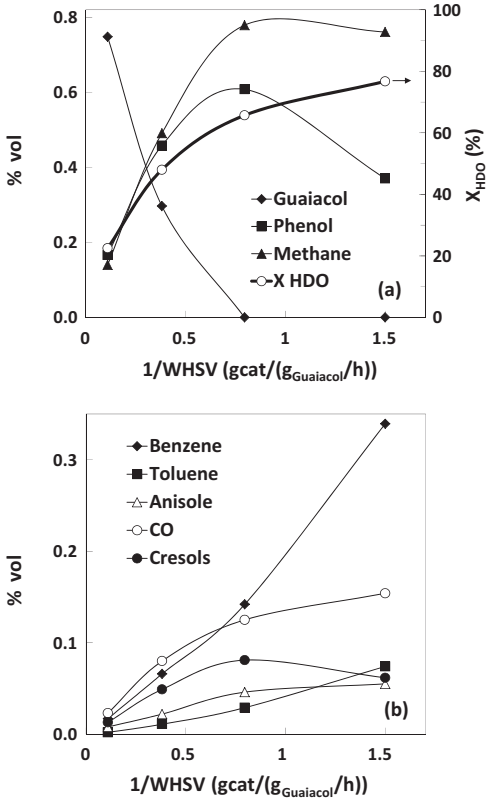

Fig. 9. Effect of WHSV on (a) molar fraction of non-reacted guaiacol and major products and on HDO conversion (see Eq. (2)), (b) molar fraction of minor products (Fe/SiO_2; 673 K; pH_2 = 0.9 bar).

HDO reactions (BTX, phenol, anisole, o-cresol) were observed with metal supported catalyst. In the absence of hydrogen, it gave isomerisation reactions. This may be ascribed to the low conversion conditions intentionally used (<12%). In similar reaction conditions, HY zeolite also exclusively gave isomerisation reactions [62].

3.5.2. Effect of temperature

Fig. 8 shows the products evolution as a function of the temperature.

Guaiacol conversion and X_{HDO}% increase with temperature (623–723 K). Benzene and toluene yield increase with temperature but also undesirable products (CH_4, CO) yield increases. The tendency to the production of higher yield in methane observed with high temperatures is consistent with thermodynamic equilibrium. However, CH_4 molar fraction remains below 1 vol.% even at 723 K, confirming the high selectivity for the range of investigated temperature. In our opinion, the influence of temperature on selectivity is a key factor considering that lignin fast pyrolysis is normally carried out at temperatures from 673 K to 873 K to increase the yield in OMAC's [20,32]. The selectivity of Fe/SiO_2 is high even with temperatures suitable to treat never-condensed pyrolysis vapours.

3.5.3. Effect of WHSV

Fig. 9 shows the effect of 1/WHSV from 0.11 to 1.50 h on products molar fraction.

Guaiacol is completely converted at 0.8 h of 1/WHSV. X_{HDO}% increased to 77% at 1.5 h (Fig. 9(a)). Phenol concentration is still quite high (0.37 vol.%) at 1/WHSV of 1.5 h whereas BT yield reaches 38%. Methane molar fraction does not increase after 0.8 h although HDO increases. At 1/WHSV of 1.5 h the molar balance of analysed aromatic rings was 84%. The fraction of not analysed rings (16%) in mono-aromatics is mainly converted to PAH and coke precursors because no ring hydrogenated products (cyclohexane and cyclohexene) were detected. Higher BT selectivity could be achieved at higher 1/WHSV by further phenols conversion. This finding justifies the interest of our simple Fe/SiO_2 catalyst that promotes HDO with little ring hydrogenation.

Phenol concentration passed through a maximum at 1/WHSV of 0.8 h. At lower WHSV, phenol is generated from guaiacol demethoxylation (see Fig. 10) and is then converted by hydrogenolysis to produce benzene and H_2O. Dehydroxylation of phenol to CO and coke production [56,57] is a minor route evidenced by carbon balance and TPO analysis.

Methane production increases with phenol production until 1/WHSV of 0.8 h (see Fig. 9(a)) showing that methane is formed from methoxyl hydrogenation (probably through methanol detected). Methane is thus not formed from phenol or ring hydrogenation (no increase of CH_4 after phenol decrease).

Anisole is detected in very low amounts. A little increase in anisole formation with 1/WHSV is observed and then anisole concentration remains constant from 0.8 h. Anisole comes from guaiacol dehydroxylation. Low concentrations of anisole as compared to phenol confirm that demethoxylation is much more favoured than dehydroxylation of guaiacol [25].

Little amounts of methyl catechol (methyl-dihydroxy-benzene) were detected, probably produced by transalkylation of guaiacol [30]. The HDO of methyl catechol produces cresols and toluene. Anisole could also be transalkylated to cresols [30].

3.5.4. Comparison between Fe/SiO_2 and Co/Kieselguhr catalyst

The commercial catalyst (Co/Kieselguhr) was tested in the same conditions as Fe/SiO_2 (varying 1/WHSV from 0.5 to 0.8 h at 673 K,

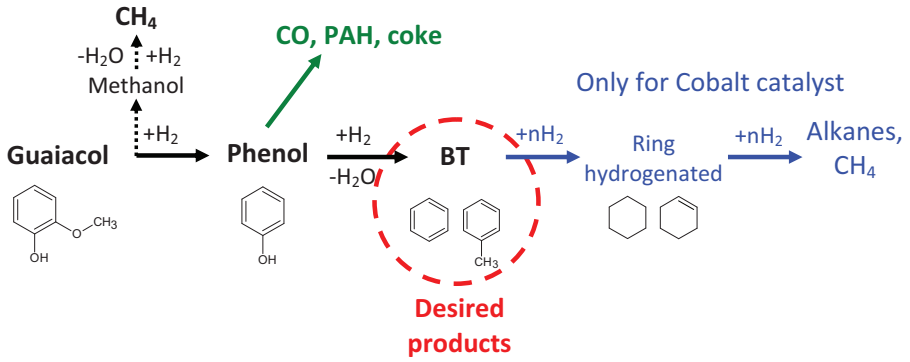

Fig. 10. Simplified chemical pathways for HDO of guaiacol over Fe/SiO_2. PAH: polycyclic aromatic hydrocarbons.

pH_2 = 0.9 bar). Product distribution was quite different. Fig. 11(a) and (b) compares both catalysts in terms of carbon yield of products.

The commercial catalyst gave higher conversions. XHDO% was 77% on Fe/SiO_2 at 1/WHSV of 1.5 h and 100% on Co/Kieselguhr at 0.8 h. However, it was less selective in the HDO reactions (Fig. 11). Indeed, Co/Kieselguhr produces very high yield in CH_4 at high X_{HDO}%, whereas Fe/SiO_2 gives a high HDO conversion with little hydrogenation of aromatic ring.

In order to compare the performance of the catalysts, the Van Krevelen [12] diagram was modified using equations 3 and 4 (Fig. 12). When Co/Kieselguhr is used, the hydrogenation of carbons happens with C—O bonds scissions. Consequently, hydrogen and carbon are consumed to produce the undesired methane. When Fe/SiO_2 is used, the diagram clearly shows that the reaction is much more directed towards the desired route and oxygen atoms are cleaved from aromatic ring without a massive hydrogenation of carbon atoms.

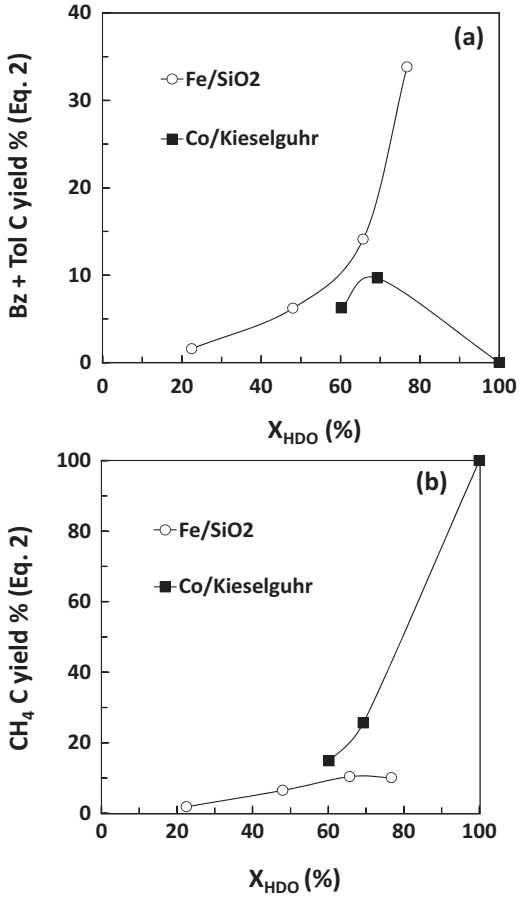

Fig. 11. Carbon yield (see Eq. (1)) of (a) benzene + toluene (goal products) and (b) methane (undesired products) as a function of HDO conversion for a range of WHSV (see Table 1) at 673 K obtained with Fe/SiO_2 and Co/Kieselguhr.

4. Discussion

It is difficult to compare our result with literature data since publications on guaiacol HDO in the gas phase are scarce and sometimes made from a different purpose than the gas-phase HDO of lignin vapours into BTX. Literature data are presented in Table 4.

Zhao et al. [24] obtained remarkable results: high BT yield (60%) at high HDO conversion (64%) using nickel phosphide. However, the optimal reaction temperature was 573 K, much lower than lignin vapours temperature. It would be interesting to analyse the performance of these catalysts at typical lignin pyrolysis vapours temperatures (673–873 K). One expects that methane production could become important on nickel-based catalyst at these temperatures. In addition (i) the contact time was much higher (20 h) than the one used in this study (1.5 h) and (ii) the concentration of guaiacol was also very low (0.024 vol.%) as compared to the concentration used in this study (1 vol.%). One has also to get in mind that nickel phosphides are expensive minerals (relative to iron) and environmentally unfriendly. Recently, Gonzalez-Borja et al. [29] tested Pt-Sn catalysts under experimental conditions close to ours. They obtained a 60% yield in BT at X_{HDO}% of 85%. The results are very interesting but Pt is a much more precious metal than iron. The deep work of Bui et al. [25,26] was inspired by catalyst already

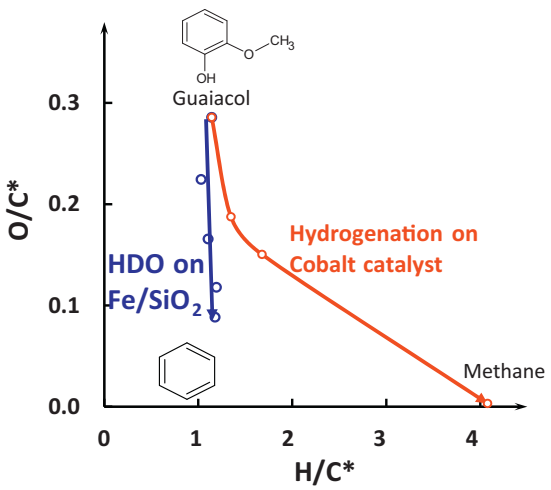

Fig. 12. Van Krevelen diagram of products (H/C* and O/C* where calculated by Eqs. (3) and (4), respectively) (Fe/SiO_2 and Co/Kieselguhr: 673 K, 0.9 bar H_2, 1/WHSV 0.11–1.50 h).

Table 4
Comparison between HDO results from literature.

Catalyst	Molecule	1/WHSV (h)	T (K)	P (atm)	Gas concentration	Products	X_{HDO}%[a]	BTX yield	References
Fe/SiO_2	Guaiacol	1.5	673	1	1% GUA; 9% Ar; 90% H_2	Benzene, Phenol, Anisole, Cresol, Toluene, CH4	74%	38%	This work
Pt-Sn/CNF	Guaiacol and anisole	3.2	673	1	0.6% GUA; 82.5%N2; 16.9% H_2	Benzene, phenol, cresol, toluene, methane, catechol	85%	60%	[29]
Ni_2P/SiO_2	Guaiacol	20.2	573	1	0.024% GUA; 80% H_2, N_2 rest	Benzene, Phenol, Anisole	64%	60%	[24]
$CoMo/ZrO_2$	Guaiacol	0.06	573	40	0.0675% GUA; 0.01% H_2S, 99.92% H_2	Phenol; benzene, methanol, catechol	28%	7%	[26]
Pt/Alumina	Guaiacol	0.1	573	1.4	3% Guaiacol, 29% H_2, 68% N_2	Phenol, dimethoxybenzene, anisole, benzene, toluene	<13%	<10%	[62]
Ni/SiO_2	Phenol	0.56	573	1	9% PhOH; 36.4% MeOH; 54.4% H_2	Benzene, cyclohexane, cyclohexene, cyclohexanone	99%	99%	[27]
Pd/CeO_2	Phenol	46.2	453	1	11.1% PhOH; 22.2% Ethanol; 66.7 H_2	Cyclohexanone, cyclohexanol	0%	0%	[28]
Pt/Hbeta (zeolite)	Anisole	0.4	673	1	2% Anisole, 98% H_2	Benzene, toluene, xylene	100%	85%	[30]

[a] Value calculated by the present author.

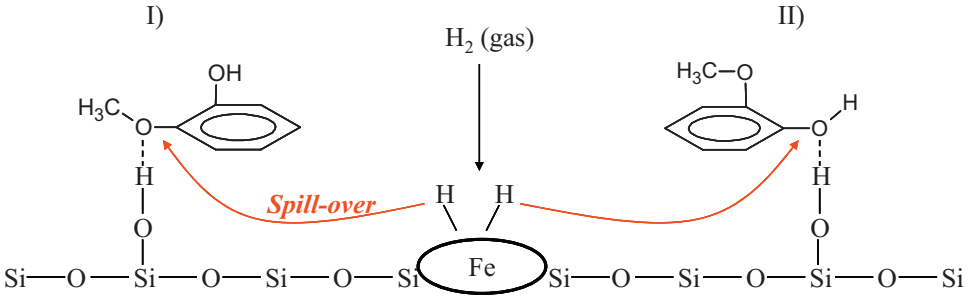

Fig. 13. Possible reaction mechanism of guaiacol conversion into aromatic hydrocarbons by HDO over Fe/SiO_2. The adsorption of guaiacol was proposed by Popov et al. [67].

proved for petroleum HDS. Unfortunately, performances obtained on CoMoS catalysts were not that expected: the HDO conversion (28%) was ~2.5 lower than in our study and the BTX yield very poor (7% against 38%) at the reaction temperature of 573 K. Nevertheless, experiments were carried out at conditions of co-feeding of biomass with fossil raw materials and on a long time on stream (40 h).

We also examined the few literature data on the catalytic gas phase hydrotreatment of phenol, the key intermediate in the studied reaction. Phenol is a solid at room temperature. Consequently many authors dissolved it in order to pump it. Shin et al. [27] investigated the influence of nickel loadings on the hydrogenation of phenol (dissolved in methanol or water) at 573 K. They found that ring hydrogenation is catalysed at low nickel loads but HDO to benzene is favoured by high nickel loadings (20%, w/w) (Table 4). The important result is the remarkable yield in benzene of 99% at 573 K. However, such performances were obtained at temperatures lower than the temperature of lignin vapours (673 K) and moreover by using methanol as an additive in the reactant flow (9% phenol; 36% methanol). Experiences reported clearly showed the important role of methanol additive in the reaction rates and products distribution [61], with and without hydrogen.

Ethanol was used instead of methanol in the hydrogenation of phenol over Pd/CeO_2 catalysts at 473 K by Velu et al. [28]. In this example, the catalysts unfortunately were totally selective to ring hydrogenation (cyclohexanone, cyclohexanol). Almost no HDO products were detected. Water was used by Shore et al. [63] with Pd and Pd-Yb silica supported catalyst. They also obtained ring hydrogenation products.

The reactivity of anisole, the second important intermediate in hydrogenation of guaiacol, has also to be discussed. Anisole HDO was investigated by Zhu et al. [30] on Pt supported on SiO_2 and HBeta zeolite at 673 K. They attained a BTX yield of 85% at X_{HDO} of 100% on Pt/HBeta zeolite. The formation of toluene and xylene is explained by anisole transalkylation. This finding is consistent with guaiacol transalkylation to methyl catechol observed in this work and by Nimmanwudipong et al. [62] on Pt/Al_2O_3. Transalkylation is thought to be catalysed by acid sites [30].

The Fe/SiO_2 system seems well suitable to the HDO of guaiacol at the reaction temperature of lignin pyrolysis vapours: high HDO conversion, fairly good yield in BTX, low aromatic ring hydrogenation and low coke deposit. As proposed in the introduction, iron is a poor hydrogenating metal towards the aromatic ring as compared to nickel or precious metals [34,35]. Silica is poorly acidic as compared to alumina [41] or some zeolites [64] and consequently lowers coke deposit from oxygenated aromatic hydrocarbons conversion [27,41].

For the hydrogenation of hydrocarbons species on metal supported catalysts, it is admitted that the reaction occurs on the support at the metal–support interface or in the vicinity of the metal particle. The substrate molecule adsorbed on acidic sites is hydrogenated by spilt-over H-species originating from the H_2 molecule dissociated on the metal particles [36,37,65,66]. With phenols-type compounds, there is a competition between the hydrogenation of the C—C aromatic bonds and the hydrogenolysis of C—O external bond. The competition can be controlled by the mode of adsorption of the phenolic molecules [26].

The interaction between phenolic compounds and silanol groups present on silica was deeply studied by means of infrared spectroscopy [67]. This study shows that the surface silanol protons interact either with the aromatic ring lying planarly on the surface or with the oxygenated groups through the O atoms.

In the guaiacol molecule, the n-electrons of the oxygen atoms are more basic than the π-electrons of C=C aromatic system. One expects that the adsorption occurs on the weak silica acidic OH sites by interaction with the O atoms (in hydroxyl or methoxy groups)

rather than with the aromatic ring. This activation favours the C—O bond breaking at the expense of the C—C bonds breaking. The chemical mechanisms are catalysed in the presence of supported iron metal particles which supply the active H-species coming from the dissociation of H_2 molecules on the metal phase. The mechanisms are schematically illustrated in Fig. 13, taking into account the findings of Popov et al. [67].

The proposed mechanism also holds for experiments carried out without hydrogen (Fig. 7). In this case, fairly good guaiacol conversion is obtained (around 30%) with low selectivity in HDO and much higher coke deposit. Since the bare support is not active in the reaction, the products formed are ascribable to the effect of the metal phase. Iron supplies the necessary active H species for the hydrogenation/hydrogenolysis reactions. These species were previously formed on the iron particles during the reduction process under hydrogen atmosphere at 773 K. The role of hydrogen reservoir of the support in metal supported catalysts is well known [66,68]. In the presence of hydrogen, more hydrogen molecules are adsorbed resulting in more active H-species on the catalyst surface, explaining the increase of HDO conversion in the presence of H_2 in the stream gas.

Phenol is formed through the adsorption mode I (the major mode) whereas anisole stems for adsorption mode II. The formation reactions also occur in contact or in the vicinity of a Fe° particle where H_2 is dissociated (Fig. 13).

It is remarkable that no catechol (2-hydroxyphenol) was detected in any experiences although it was shown that catechol is easier to produce than anisole by analysing guaiacol bond energies [25]. Kinetic barriers may exist for catechol formation. It is also possible that catechol, once formed, stays strongly adsorbed to silica support and desorption will be much slower than HDO reaction.

Bronsted acid sites are also responsible of transalkylation [64]. Methyl catechol (2-hydroxy methyl benzene) was detected in some experiences. It can be produced by transalkylation of guaiacol [62]. Further HDO of methyl catechol explains the formation of cresols and toluene.

5. Conclusion

Fe/SiO_2 was shown to be an active and selective catalyst for the conversion of guaiacol into aromatic hydrocarbons at temperatures as high as 673 K matching with the temperature of never-condensed lignin pyrolysis vapours. Hydrogen partial pressure (0.2–0.9 bar) affects product distribution only slightly. Temperature (623–723 K) accelerates reaction rate without big changes in the selectivity. The lower activity of Fe/SiO_2 compared with Co-based catalyst is offset by a higher HDO selectivity on a wider range of temperature. Moreover, Fe/SiO_2 produces less methane than the commercial cobalt-based catalyst even at high HDO conversions. Fe/SiO_2 could be a more versatile catalyst easier to be operated in catalytic reactors. It has also the advantage of being inexpensive and environmentally friendly. It could be a potential catalyst for lignin to BTX production process by lignin fast pyrolysis followed by HDO of the vapours. HDO conversion of 74% and BT yield of 38% was achieved in the best investigated conditions.

Works are still needed to investigate the effect of other gases and tars generated by lignin pyrolysis and to optimise this catalyst. The commercial application of lignin to BTX processes will depend on the development of suitable technologies for lignin conversion and vapours catalytic up-grading and on the evolution of BTX prices nowadays produced from crude oil.

Acknowledgements

The CNRS (Centre National de la Recherche Scientifique, France)-Programme Interdisciplinaire Energie (« CRAKIN » project) and the MESR (Ministère de l'Enseignement Supérieur et de la Recherche, France) are acknowledged for financial supports. The workshop of LRGP-CNRS, Olivier Herbinet (LRGP-ENSIC), and Michel Mercy (SRSMC-UHP) are kindly acknowledged for technical supports. P.A. Glaude (LRGP-CNRS) is also acknowledged for his advice on thermodynamic calculations.

Appendix A. Supplementary data

Supplementary data associated with this article can be found, in the online version, at doi:10.1016/j.apcatb.2011.12.005.

References

[1] J. Zakzeski, P. Bruijnincx, A. Jongerius, B. Weckhuysen, Chem. Rev. 110 (6) (2010) 3552.
[2] J. Holladay, J. Bozell, J. White, D. Johnson, Top value-added chemicals from biomass, vol. II, Report of the PNNL, US Department of Energy (2007).
[3] J. Van Haveren, E. Scott, J. Sanders, Biofuels Bioprod. Bioref. 2 (2008) 41.
[4] B. Kamm, M. Kamm, Appl. Microbiol. Biotechnol. 64 (2004) 137.
[5] Kirk-Othmer Encyclopedia, 4th edition, 1993.
[6] T.R. Carlson, Y-T. Cheng, J. Jae, G.W. Huber, Energy Environ. Sci. 4 (2011) 145.
[7] M. Jackson, D. Comption, A. Boateng, J. Anal. Appl. Pyrolysis 85 (2009) 226.
[8] C. Mullen, A. Boateng, Fuel Proc. Technol. 91 (2010) 1446.
[9] K. Murata, Y. Liu, M. Inaba, I. Takahara, Catal. Lett. 140 (2010) 8.
[10] R.W. Thring, S.P.R. Katikaneni, N. Bakhshi, Fuel Proc. Technol. 62 (2000) 17.
[11] R. French, S. Czernik, Fuel Proc. Technol. 91 (2010) 25.
[12] P. de Wild, R. Van der Laan, A. Kloekhorst, E. Heeres, Environ. Prog. Sust. Energy 28 (3) (2009) 461.
[13] J. Shabtai, W. Zmierczak, E. Chornet, D. Johnson, US Patent 2003/0115792 A1.
[14] J. Shabtai, E. Chornet, W. Zmierczak, US Patent 5959167 (1998).
[15] P. Urban, D. Engel, US Patent 4731491 (1988).
[16] H. Parkhurst, D. Huibers, M. Jones, Preprints of ACS Symposium, 1980, pp. 657–667.
[17] G.W. Huber, S. Iborra, A. Corma, Chem. Rev. 106 (2006) 4044.
[18] C. Amen-Chen, H. Pakdel, C. Roy, Bioresour. Technol. 79 (2001) 277.
[19] D. Shen, S. Gu, K. Luo, S. Wang, M. Fang, Bioresour. Technol. 101 (2010) 6136.
[20] O. Faix, D. Meier, I. Grobe, J. Anal. Appl. Pyrolysis 11 (1987) 403.
[21] E. Laurent, B. Delmon, Appl. Catal. A 109 (1994) 77.
[22] A. Oasmaa, A. Johansson, Energy Fuels 7 (1993) 426.
[23] D. Elliot, T. Hart, Energy Fuels 23 (2009) 631.
[24] H. Zhao, D. Li, P. Bui, S. Oyama, Appl. Catal. A 391 (2011) 305.
[25] V. Bui, G. Toussaint, D. Laurenti, C. Mirodatos, C. Geantet, Catal. Today 143 (2009) 172.
[26] V. Bui, D. Laurenti, P. Delichère, C. Geantet, Appl. Catal. B 101 (2011) 246.
[27] E.-J. Shin, M. Keane, Ind. Eng. Chem. Res. 39 (2000) 883.
[28] S. Velu, M. Kapoor, S. Inagaki, K. Suzuki, Appl. Catal. A 245 (2003) 317.
[29] M. Gonzalez-Borja, D. Resasco, Energy Fuels 25 (9) (2011) 4155.
[30] X. Zhu, L. Lobban, R. Mallinson, D. Resasco, J. Catal. 281 (2011) 21.
[31] J. Adjaye, N. Bakhshi, Fuel Proc. Technol. 45 (1995) 161.
[32] D. Nowakowski, A. Bridgwater, D. Elliott, D. Meier, P. de Wild, J. Anal. Appl. Pyrolysis 88 (2010) 53.
[33] T. Faravelli, A. Frassoldati, G. Migliavacca, E. Ranzi, Biomass Bioenergy 34 (2010) 290.
[34] P. Emmett, N. Skau, J. Am. Chem. Soc. 65 (1943) 1029.
[35] K. Yoon, A. Vannice, J. Catal. 82 (1983) 457.
[36] S.D. Lin, M.A. Vannice, J. Catal. 143 (1993) 539.
[37] S.D. Lin, M.A. Vannice, J. Catal. 143 (1993) 554.
[38] M. Houalla, B. Delmon, J. Phys. Chem. 84 (1980) 2194.
[39] S.P. Noskova, M.S. Borisova, V.A. Dzisko, Kinet. Katal. 16 (2) (1975) 497.
[40] C.H. Bartholomew, R.J. Farrauto, J. Catal. 45 (1976) 41.
[41] A. Centeno, E. Laurent, B. Delmon, J. Catal. 154 (1995) 288.
[42] M. Huuska, J. Rintala, J. Catal. 94 (1985) 230.
[43] M. Ferrari, S. Bosmans, R. Maggi, B. Delmon, P. Grange, Catal. Today 65 (2001) 257.
[44] M. Ferrari, B. Delmon, P. Grange, Microporous Mesoporous Mater. 56 (2002) 279.
[45] A. Jasik, R. Wojcieszak, S. Monteverdi, M. Ziolek, M. Bettahar, J. Mol. Catal. A 242 (2005) 81.
[46] V. Yakovlev, S. Khromova, O. Sherstyuk, V. Dundich, D. Ermakov, V. Novopashina, M. Lebedev, O. Bulavchenko, V. Parmon, Catal. Today 144 (2009) 362.
[47] R.N. Olcese, M. Bettahar, D. Petitjean, J-C. Moise, A. Dufour, First International Congress on Catalysis for Biorefineries (CatBior), Torremolinos-Málaga, Spain, 2011.
[48] http://www.c.morley.dsl.pipex.com/ (visited 1.10.2011).
[49] C. Muller, V. Michel, G. Scacchi, G.M. Come, J. Chim. Phys. 95 (1995) 1154.
[50] CEN/BT/TF 143, Biomass Gasification—Tar and Particles in Product Gases—Sampling and Analysis, CEN, Brussels, 2005, p. 42.
[51] A. Dufour, P. Girods, E. Masson, S. Normand, Y. Rogaume, A. Zoulalian, J. Chromatogr. A 1164 (2007) 240.

[52] J. Carignan, P. Hild, G. Mevelle, J. Morel, D. Yeglicheyan, Geostandard Newslett. 25 (2001) 187.
[53] J. Rodriguez-Carvajal, B. Physica, Phys. Condens. Matter 192 (1993) 55.
[54] G. Le Caer, IJL-CNRS, private communication.
[55] A. Dufour, A. Celzard, B. Ouartassi, F. Broust, V. Fierro, A. Zoulalian, Appl. Catal. A 360 (2009) 120.
[56] R. Cypres, Fuel Proc. Technol. 15 (1987) 1.
[57] A. Dufour, E. Masson, P. Girods, Y. Rogaume, A. Zoulalian, Energy Fuels 25 (9) (2011) 4182.
[58] http://rruff.geo.arizona.edu/AMS/amcsd.php (visited 1.10.2011).
[59] P. Decyk, M. Trejda, M. Ziolek, J. Kujawa, K. Głaszczka, M. Bettahar, S. Monteverdi, M. Mercy, J. Catal. 219 (2003) 146.
[60] B.Valle, A. Gayubo, A. Aguayo, M. Olazar, J. Bilbao, Energy Fuels 24 (2010) 2060.
[61] E. Shin, M. Keane, J. Catal. 173 (1998) 450.
[62] T. Nimmanwudipong, R. Runnebaum, D. Block, B. Gates, Catal. Lett. 141 (2011) 779.
[63] S. Shore, E. Ding, C. Park, M. Keane, Catal. Commun. 3 (2002) 77.
[64] C. Perego, S. Amarilli, A. Carati, C. Flego, G. Pazzuconi, C. Rizzo, G. Bellussi, Microporous Mesoporous Mater. 27 (1999) 345.
[65] F. Benseradj, F. Sadi, M. Chater, Appl. Catal. A 228 (2002) 135.
[66] W.C. Conner, J.L. Falconer, Chem. Rev. 95 (1995) 759.
[67] A. Popov, E. Kondratieva, J. Goupil, L. Mariey, P. Bazin, J. Gilson, A. Travert, F. Mauge, J. Phys. Chem. C 114 (2010) 15661.
[68] R. Wojcieszak, S. Monteverdi, J. Ghanbaja, M.M. Bettahar, J. Colloid Interface Sci. 317 (2008) 166.